Supporting Information

Exploiting nucleobase-containing materials – from monomers to complex morphologies using RAFT dispersion polymerization

Yan Kang,[a] Anaïs Pitto-Barry,[a] Helen Willcock,[a] Wendong Quan,[a] Nigel Kirby,[b] Ana M. Sanchez[c] and Rachel K. O'Reilly*[a]

[a] Department of Chemistry, University of Warwick, Library Rd., Coventry, CV4 7AL, U.K. E-mail: Rachel.oreilly@warwick.ac.uk
[b] Australian Synchrotron, 800 Blackburn Road, Clayton VIC 3168, Australia
[c] Department of Physics, University of Warwick, Library Rd., Coventry, CV4 7AL, U.K.

Contents

Section 1. ^{1}H NMR spectrum and SEC analysis of PMMA macro-CTA, **1**

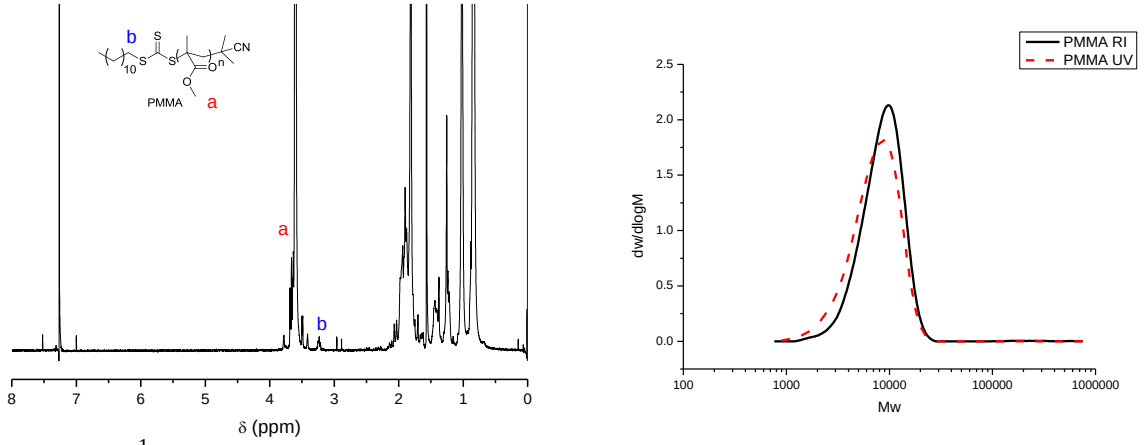

Figure S1. ^{1}H NMR spectrum in $CDCl_3$ (left) and SEC trace (right, DMF as eluent, PMMA standards) of PMMA, **1**.

Section 2. SEC analysis of polymers **1-11**

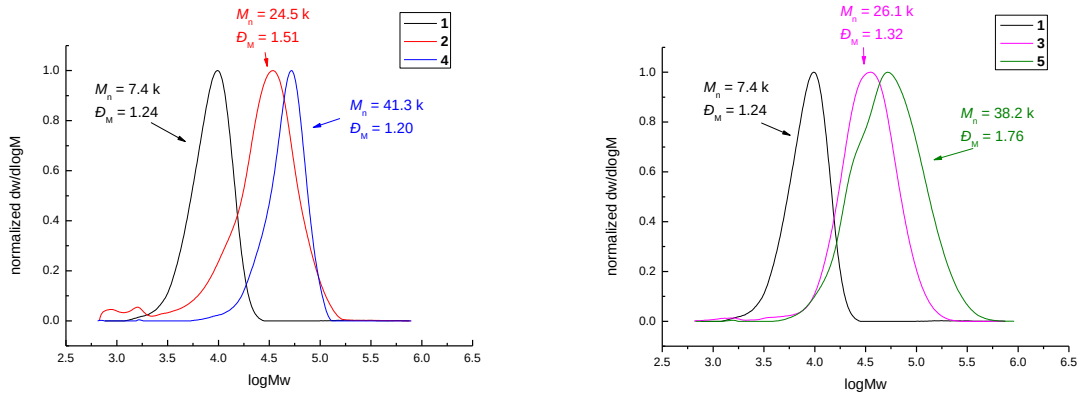

Figure S2. SEC traces of polymers **1-5** prepared by RAFT dispersion polymerization in $CHCl_3$. (DMF as eluent, PMMA standards).

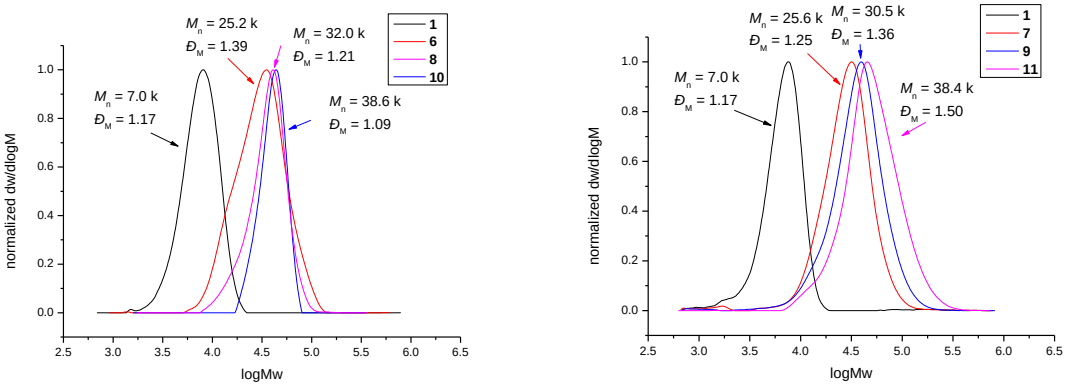

Figure S3. SEC traces of polymers **1**, **6-11** prepared by RAFT dispersion polymerization in 1,4-dioxane. (DMF as eluent, PMMA standards).

Section 3. Kinetics of polymerization **3**

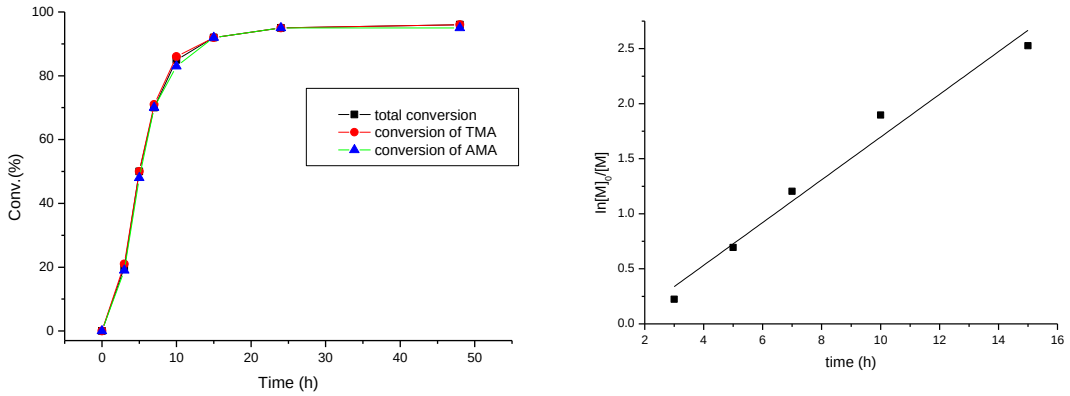

Figure S4. Conversion vs. time plot and corresponding semi-logarithmic plot obtained for the dispersion polymerization of a mixture of AMA and TMA at 60 ^{o}C using a PMMA macro-CTA in $CHCl_3$.

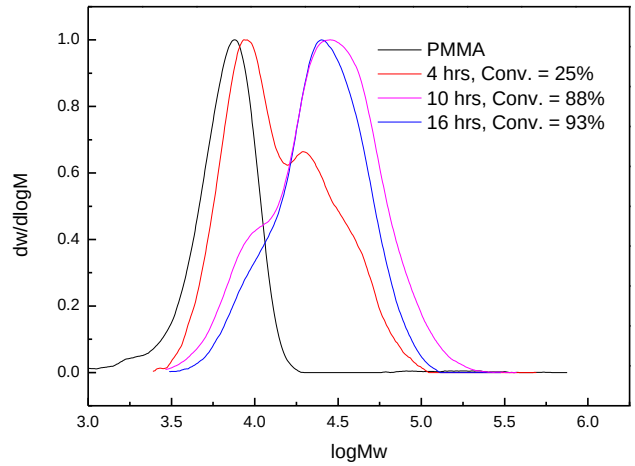

Figure S5. SEC traces and their corresponding monomer conversions obtained from separate RAFT dispersion polymerizations, which were stopped at different reaction time. Note that the condition of the RAFT dispersion polymerization is as same as it used for the kinetics study of **3**.

Section 4. TEM and SANS analysis of self-assembly afforded by **3**

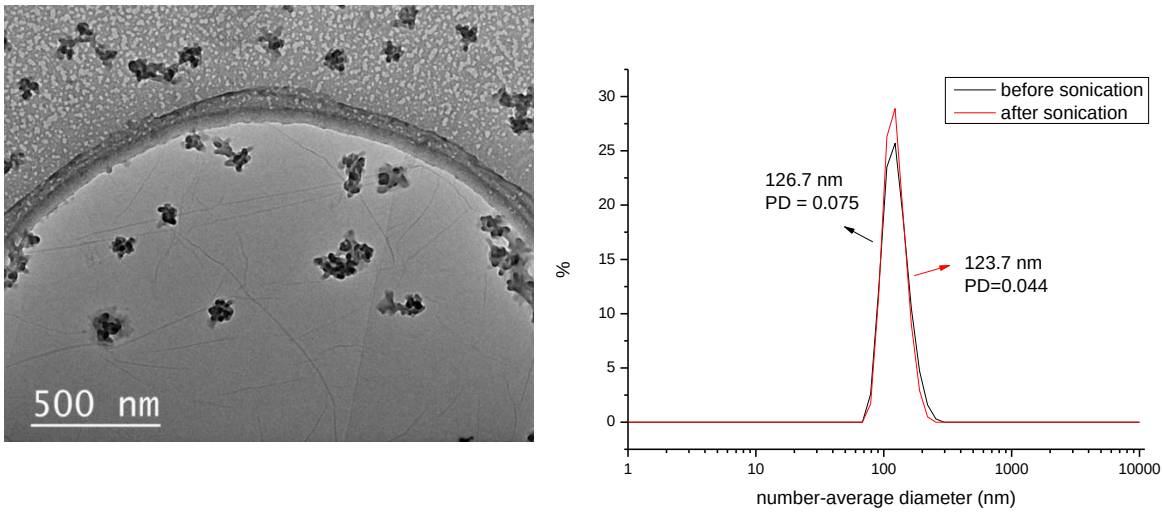

Figure S6. TEM and DLS of self-assembly prepared by **3** upon sonication for 1 hour.

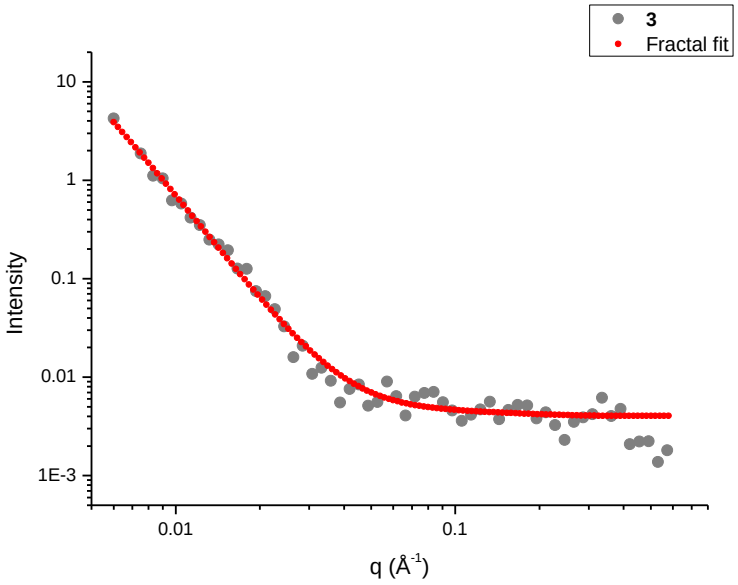

Figure S7. SANS experiment profile and fitting of the solution of **3** with a fractal model.

Section 5. Additional studies at higher DP of PAMA block

Table S1. Characterizaion data of PAMA with higher DP

Polymer/polymerization	Conv. (%)	$M_{n,th}$ (kDa)	$M_{n,NMR}$ (kDa)	$M_{n,SEC}$ (kDa)	$Đ_M$	TEM, DLS
$PMMA_{70}$-*b*-$PAMA_{150}$	85	45.2	44.5	38.3	1.27	Figure S8
$PMMA_{70}$-*b*-$PAMA_{200}$	85	58.0	54.0	38.6[a]	1.35[a]	Figure S9

[a.] Polymer is not fully soluble in DMF.

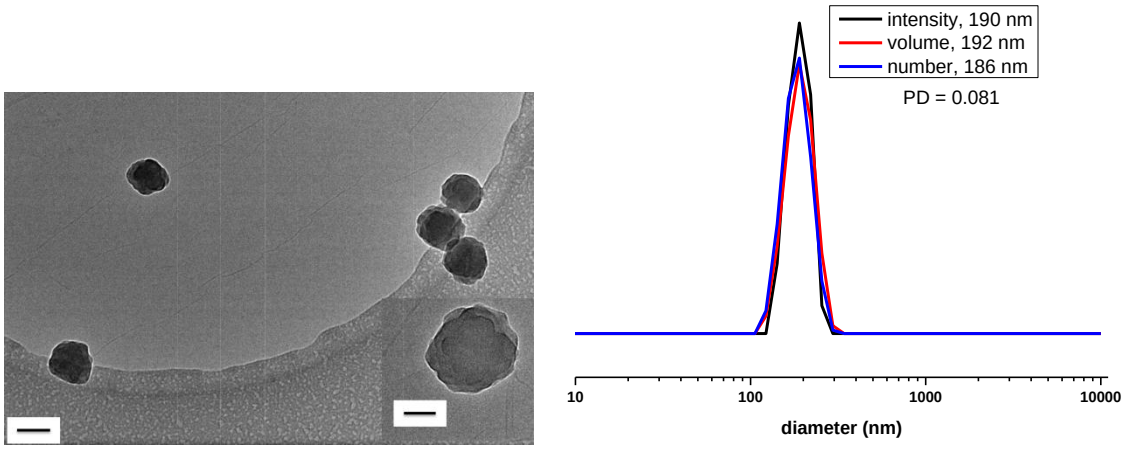

Figure S8. TEM and DLS analysis of target polymer $PMMA_{70}$-*b*-$PAMA_{150}$. Scale bar 100 nm (inset: 50 nm)

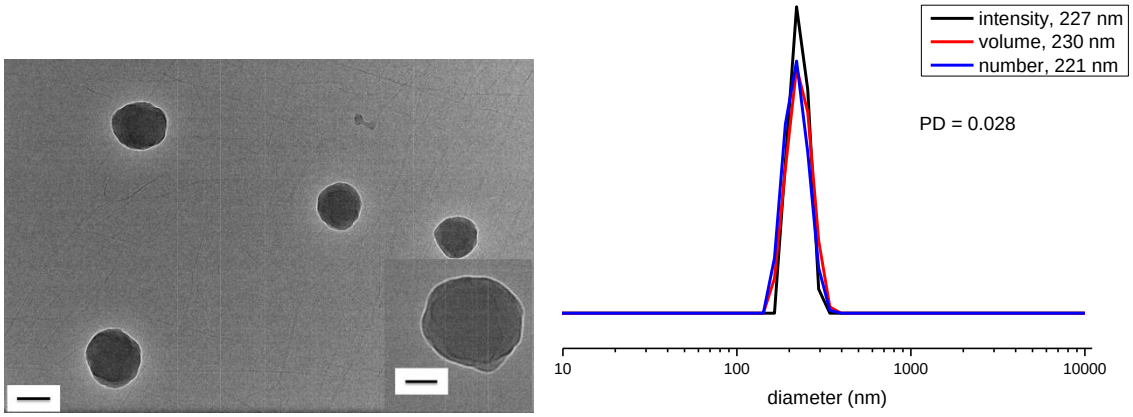

Figure S9. TEM and DLS analysis of target polymer $PMMA_{70}$-*b*-$PAMA_{200}$. Scale bar 100 nm (inset: 50 nm)

Section 6. Study of the formation of staggered lamella in the presence of anisole for the target polymers $PMMA_{70}$-*b*-$(PAMA_x$-*co*-$PTMA_y)_{100}$

Table S2 Characterization of polymers synthesized in the presence of anisole

Polymerization /polymer	Solvent ($CHCl_3$: anisole)	Monomers	Conv. (%)	$M_{n,th}$ (kDa)	$M_{n,NMR}$ (kDa)	$M_{n,SEC}$ (kDa)	$Đ_M$	TEM/DLS
a	5:1	AMA	85	32.5	33.0	32.8	1.27	Figure S10
b	1:1	Mixture of AMA and TMA (1:1)	Precipitation occured					

c	2:1	Mixture of AMA and TMA (1:1)	90	34.0	35.0	37.6	1.48	Figure S11
d	5:1	Mixture of AMA and TMA (1:1)	98	36.4	37.0	38.2	1.58	Figure S12

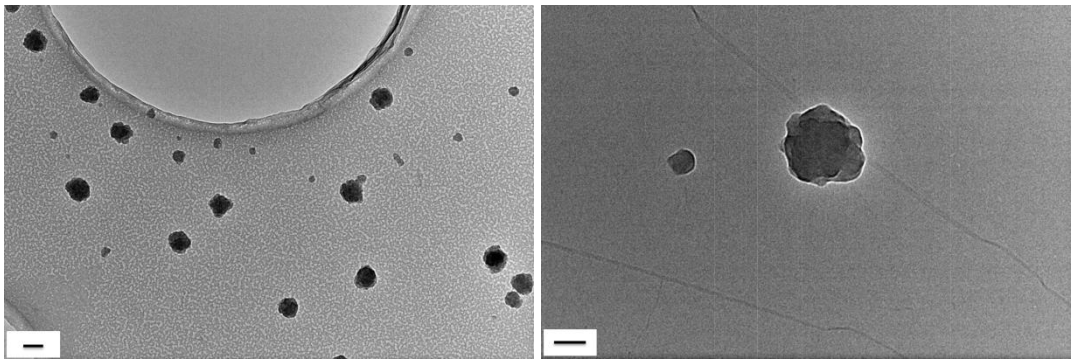

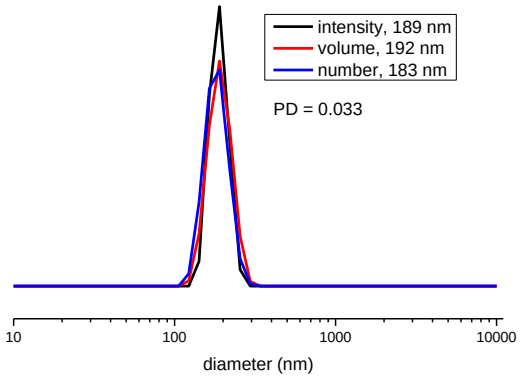

Figure S10**.** TEM, and DLS analysis of target polymer **a** in a mixture of chloroform and anisole (5:1). Scale bar left: 100 nm; right: 50nm

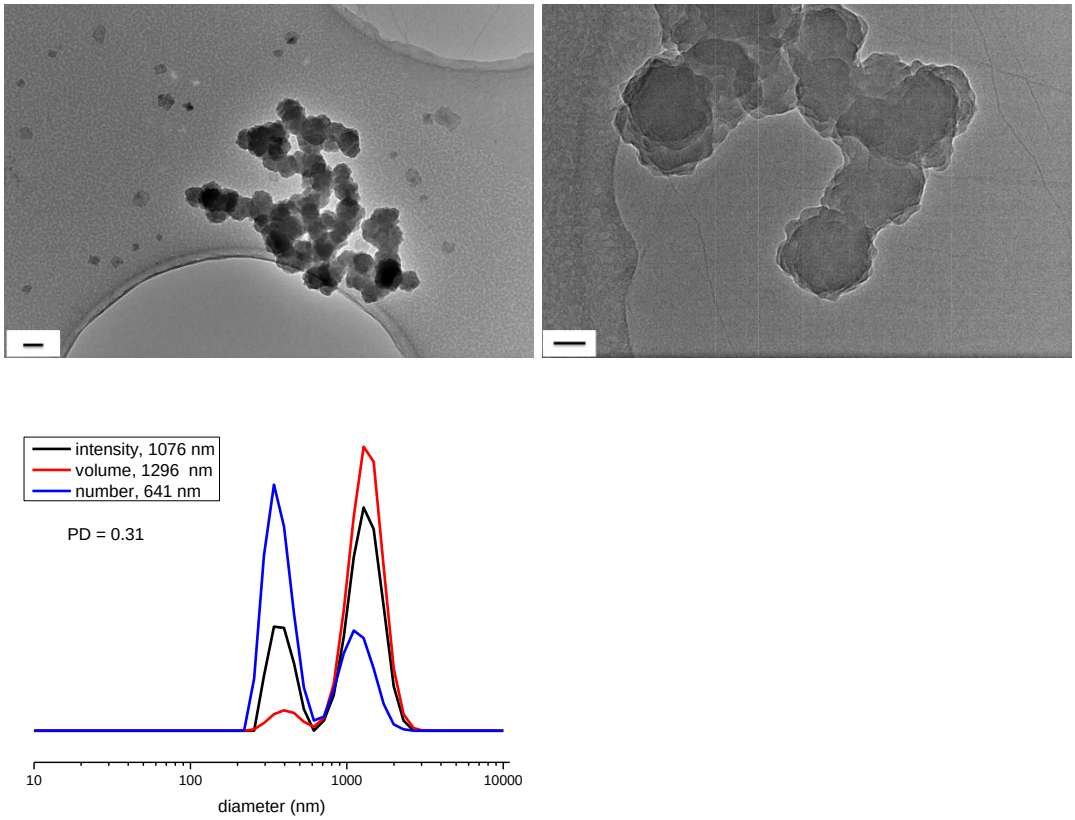

Figure S11. TEM and DLS analysis of target polymer **c** in a mixture of chloroform and anisole (2:1). Scale bar left:100 nm; right: 50 nm

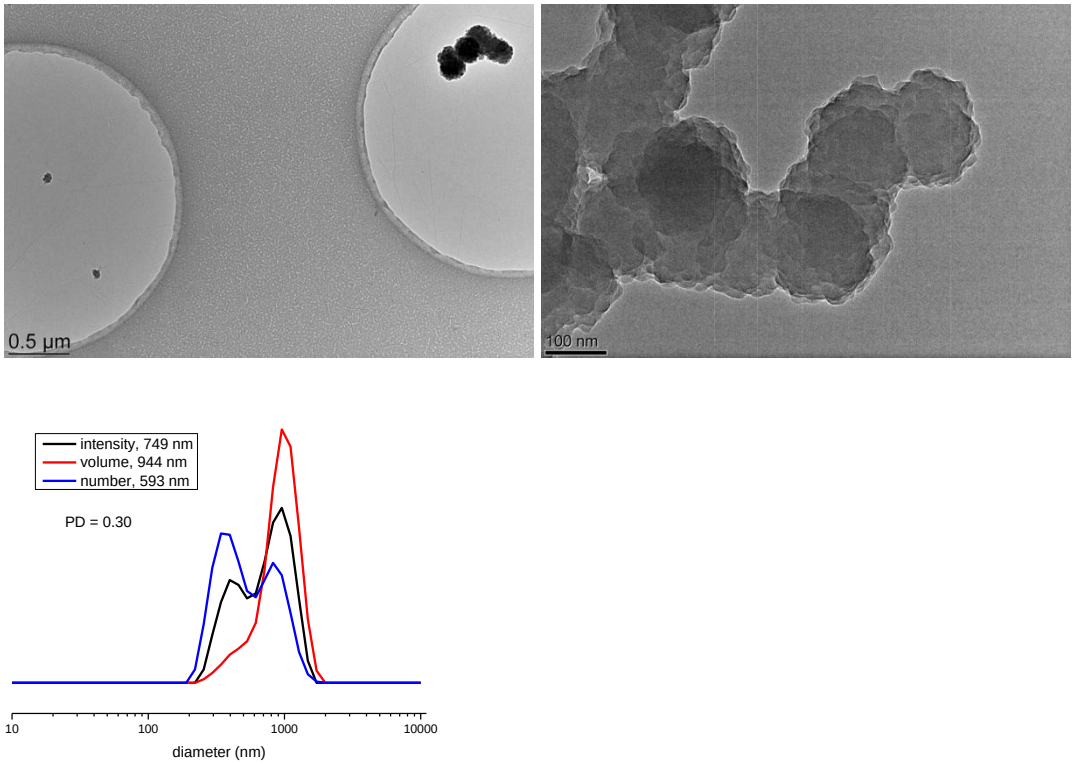

Figure S12. TEM and DLS analysis of target polymer **d** in a mixture of chloroform and anisole (5:1).

Section 7. AFM, variable-temperature DLS, SLS analysis of self-assembly afforded by **3** at different temperatures (20 ^{o}C and 50 ^{o}C)

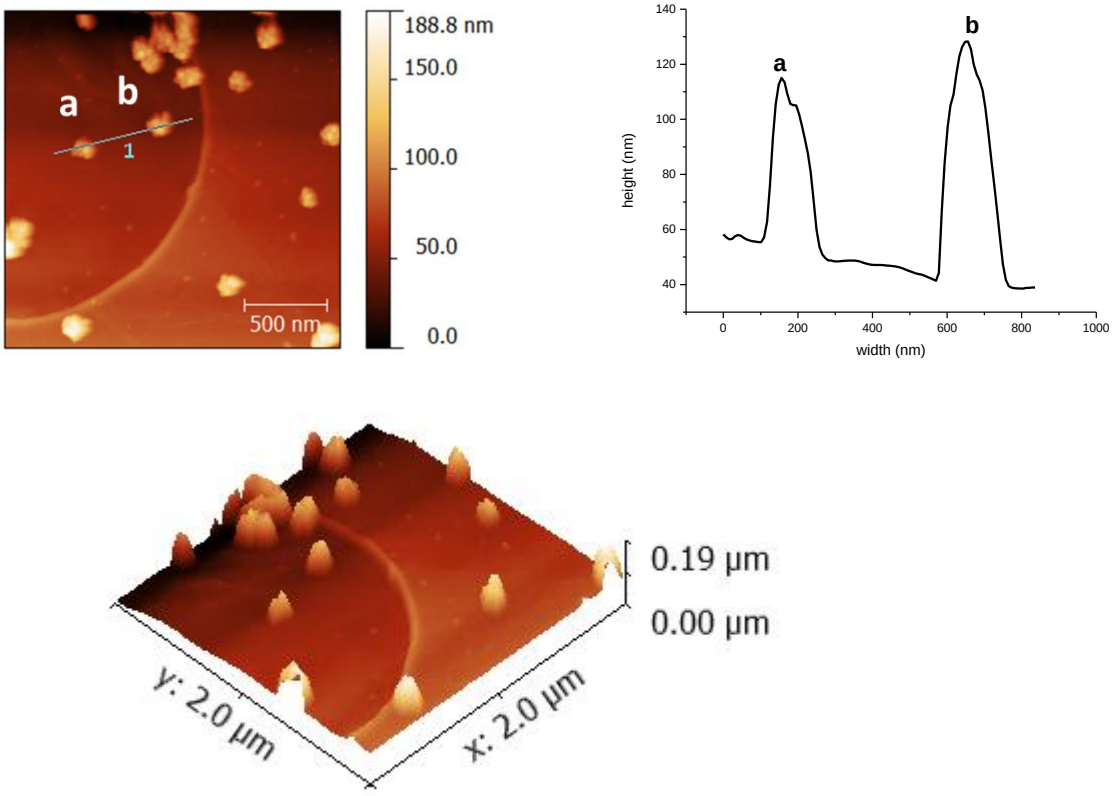

Figure S13. AFM height image (top left) and three-dimensional AFM image (bottom) of self-assembly prepared by polymerization **3** and the corresponding height profile (top right).

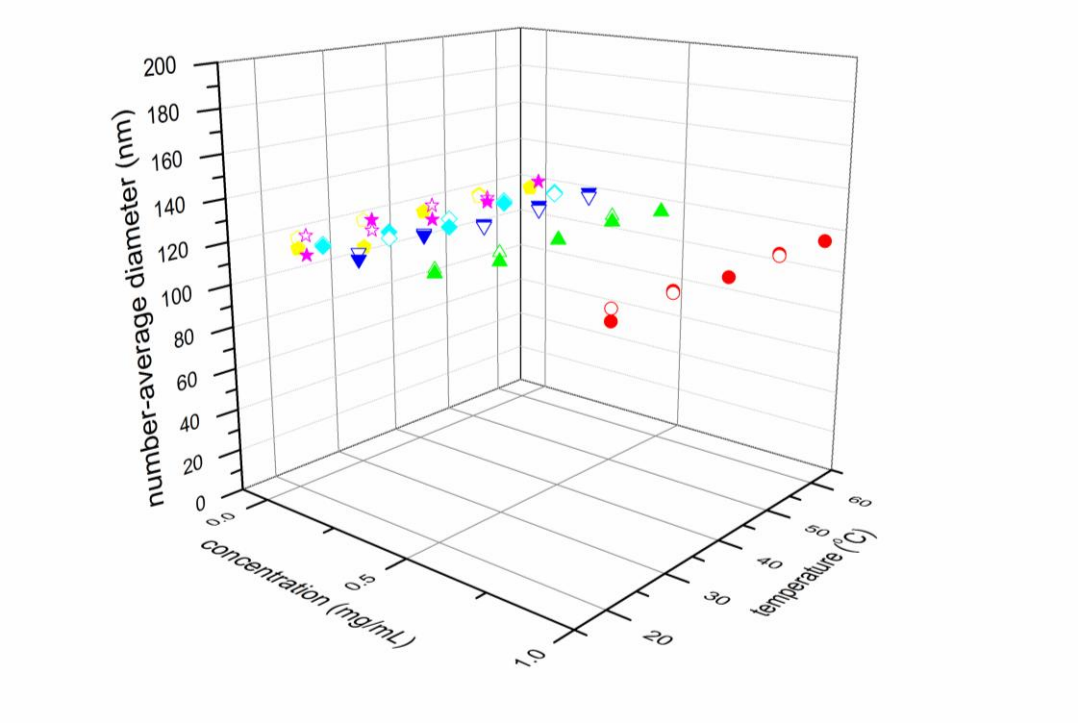

Figure S14. Number-average diameters of self-assembly with different concentrations of polymerization **3** at different temperatures measured by variable temperature DLS (hollow symbol is for heating cycle; solid symbol is for cooling cycle).

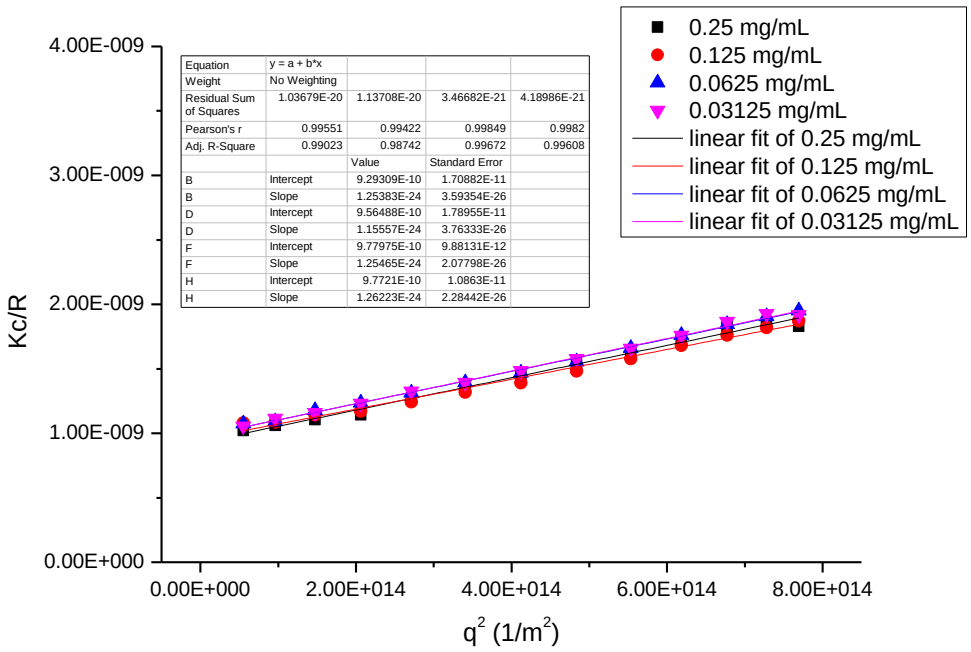

Equation	y = a + b*x			
Weight	No Weighting			
Residual Sum of Squares	1.03679E-20	1.13708E-20	3.46682E-21	4.18986E-21
Pearson's r	0.99551	0.99422	0.99849	0.9982
Adj. R-Square	0.99023	0.98742	0.99672	0.99608
		Value	Standard Error	
B	Intercept	9.29309E-10	1.70882E-11	
B	Slope	1.25383E-24	3.59354E-26	
D	Intercept	9.56488E-10	1.78955E-11	
D	Slope	1.15557E-24	3.76333E-26	
F	Intercept	9.77975E-10	9.88131E-12	
F	Slope	1.25465E-24	2.07798E-26	
H	Intercept	9.7721E-10	1.0863E-11	
H	Slope	1.26223E-24	2.28442E-26	

Figure S15. Zimm plots for self-assembly prepared by polymerization **3** measured by SLS at 20 ^{o}C.

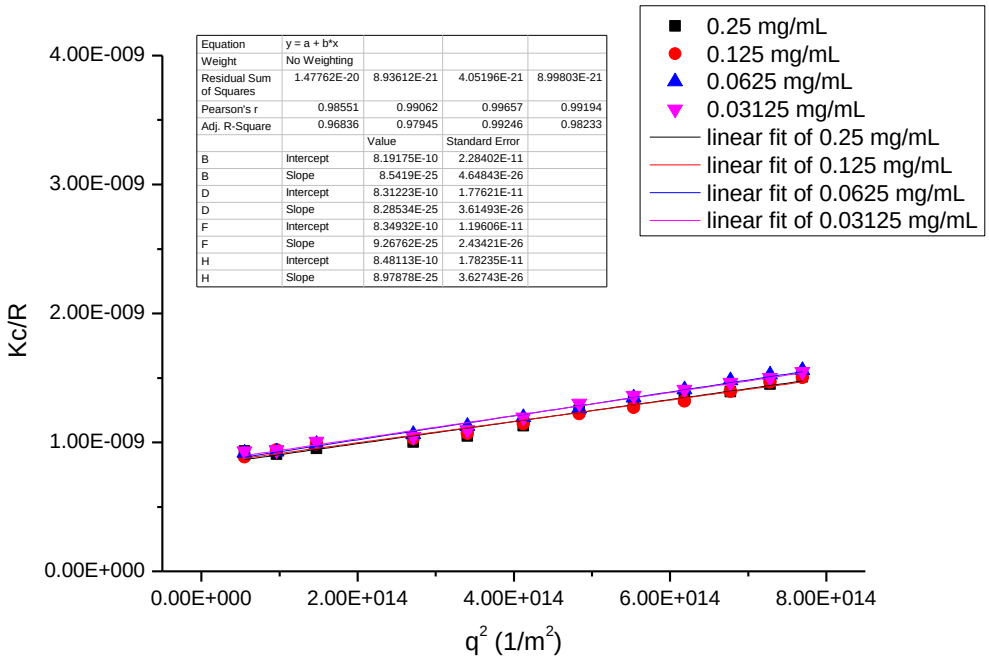

Figure S16. Zimm plots for self-assembly prepared by polymerization **3** measured by SLS at 50 ^{o}C.

Section 8. Stablity study on self-assembly **2** and **5** upon heating and ultrasonication determined by variable temperature DLS and TEM

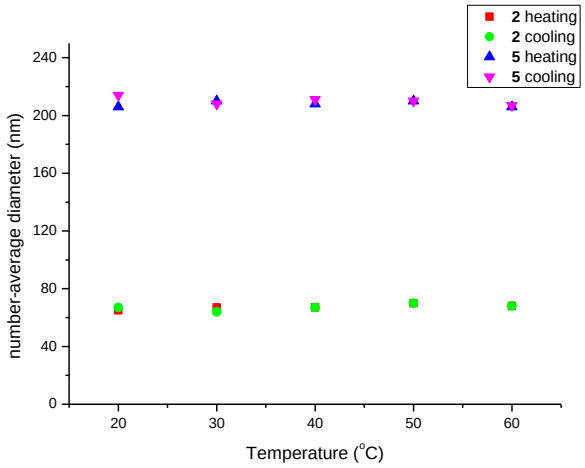

Figure S17. Number-average diameters of self-assembly of polymerization **2** and **5** at different temperatures measured by variable temperature DLS.

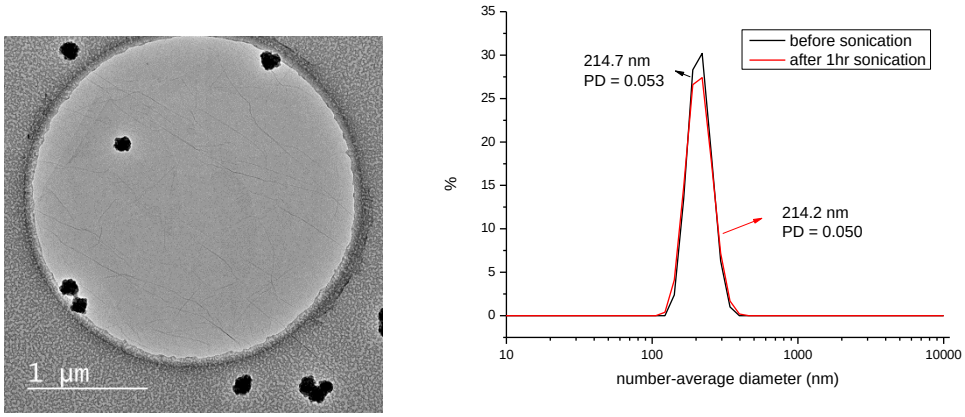

Figure S18. TEM and DLS of self-assembly prepared by polymerization **5** upon sonication for 1 hour.

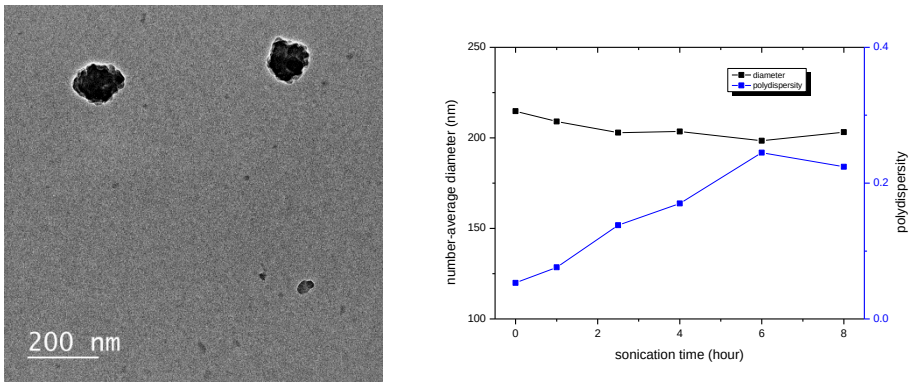

Figure S19. TEM and DLS of self-assembly prepared by polymerization **5** upon sonication for 8 hour.

Section 9. Kinetics of polymerization **7**

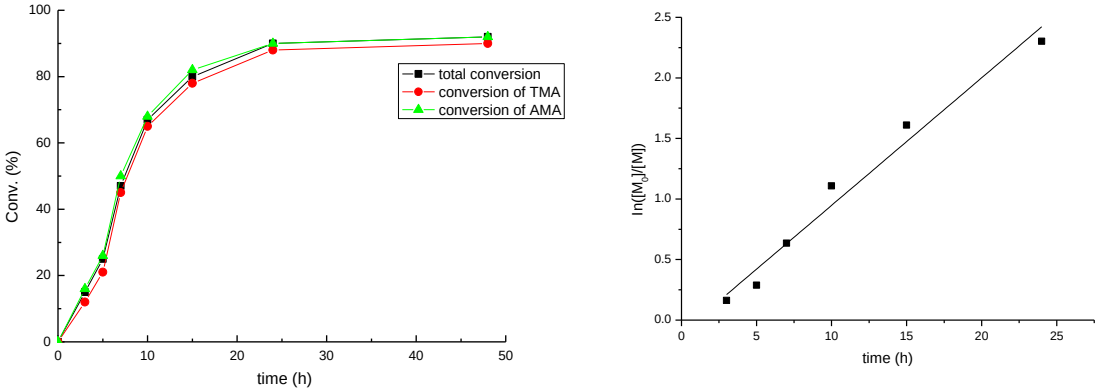

Figure S20. Conversion vs. time plot and corresponding semi-logarithmic plot obtained for the dispersion polymerization of a mixture of AMA and TMA at 60 ^{o}C using a PMMA macro-CTA in 1,4-dioxane.

Section 10. SAXS analysis of self-assembly afforded by **7**

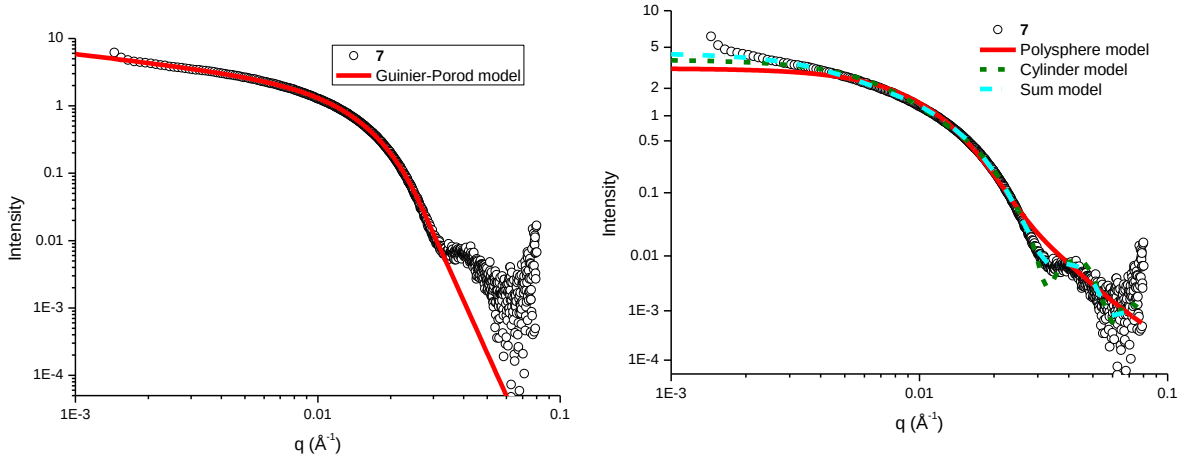

Figure S21. SAXS analysis of polymer **7**. Experimental profile and Guinier-Porod fit (left); experimental profile and fits with sphere, cylinder and sum models (right).

Section 11. AFM and SAXS analysis of self-assembly afforded by **6**

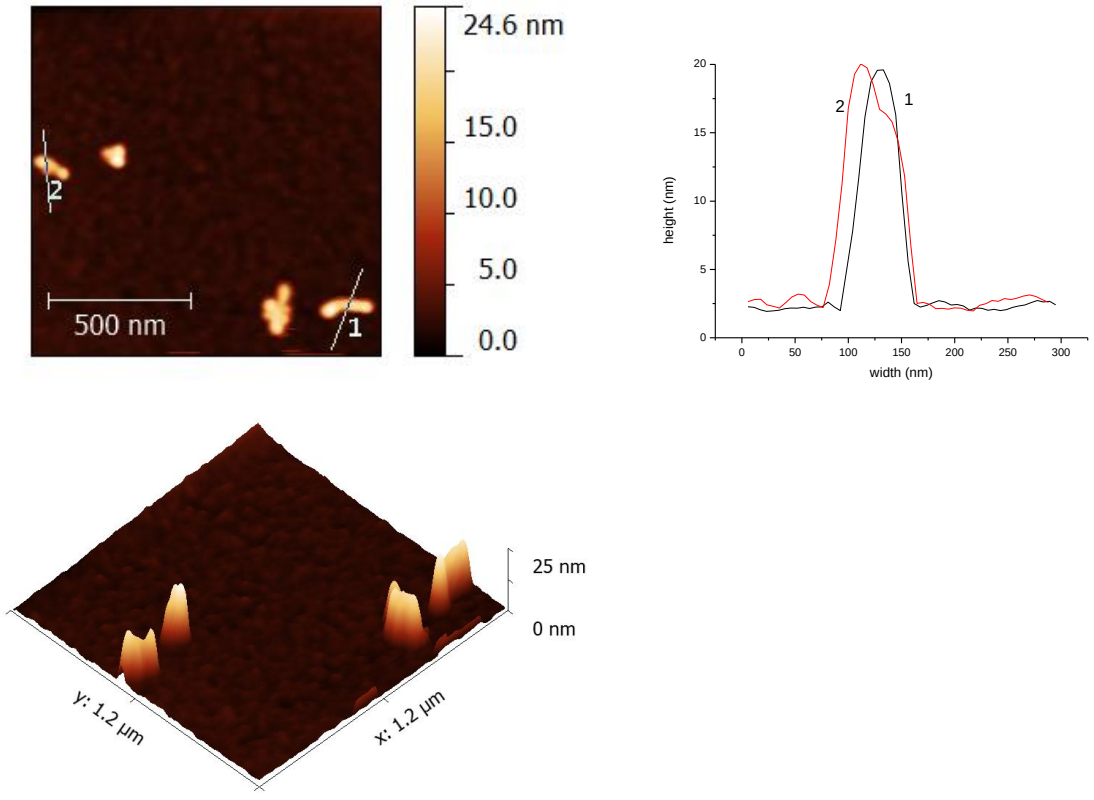

Figure S22. AFM height image (top left) and three-dimensional AFM image (bottom) of self-assembly prepared by polymerization **6** and the corresponding height profile (top right).

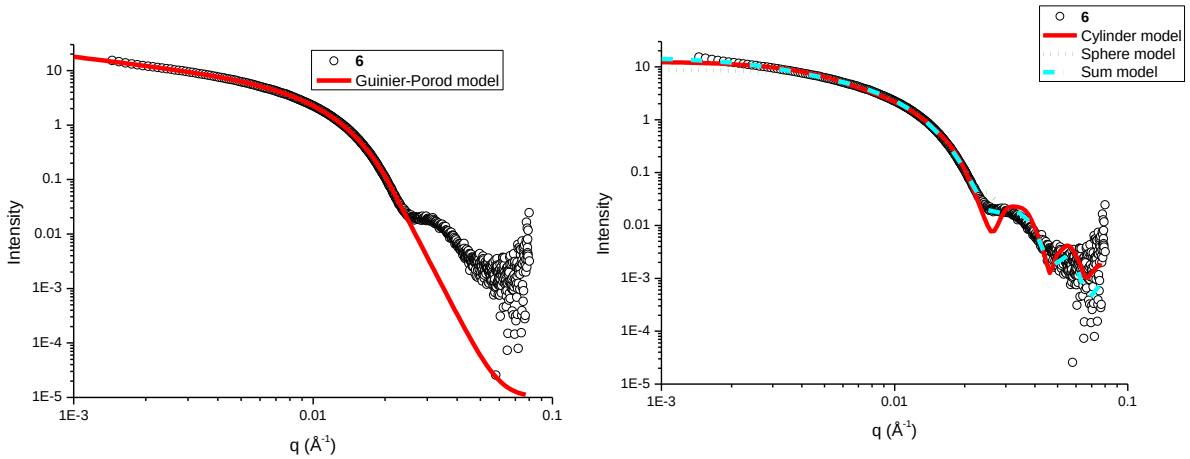

Figure S23. SAXS analysis of polymer **6**. Experimental profile and Guinier-Porod fit (left); experimental profile and fits with sphere, cylinder and sum models (right).

Section 12. AFM analysis of self-assembly afforded by **8**

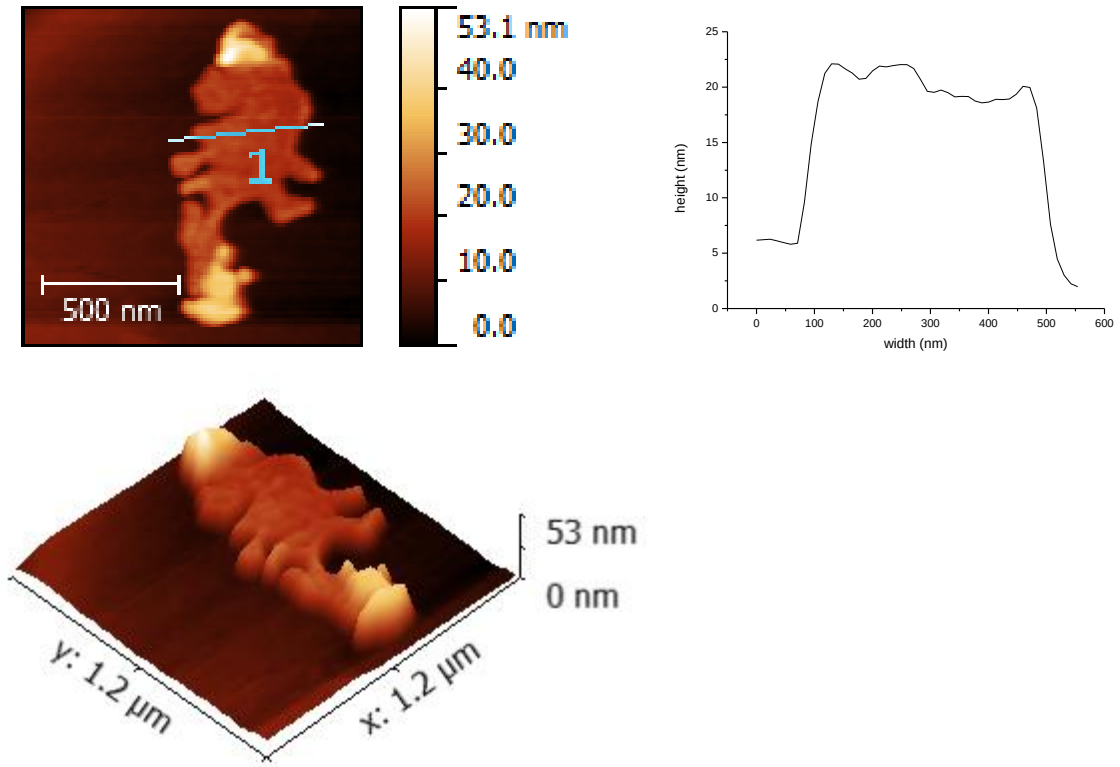

Figure S24. AFM height image (top left) and three-dimensional AFM image (bottom) of self-assembly prepared by polymerization **8** and the corresponding height profile (top right).

Section 13. AFM and SLS analysis of self-assembly afforded by **10**

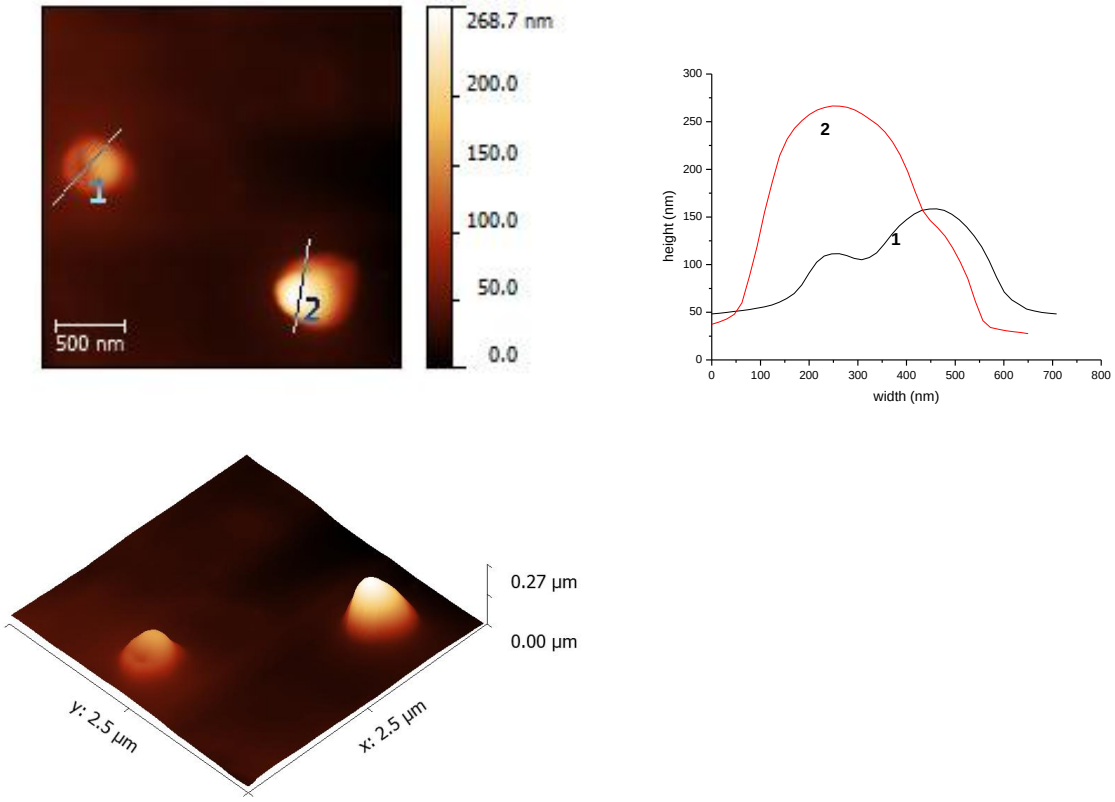

Figure S25. AFM height image (top left) and three-dimensional AFM image (bottom) of self-assembly prepared by polymerization **10** and the corresponding height profile (top right).

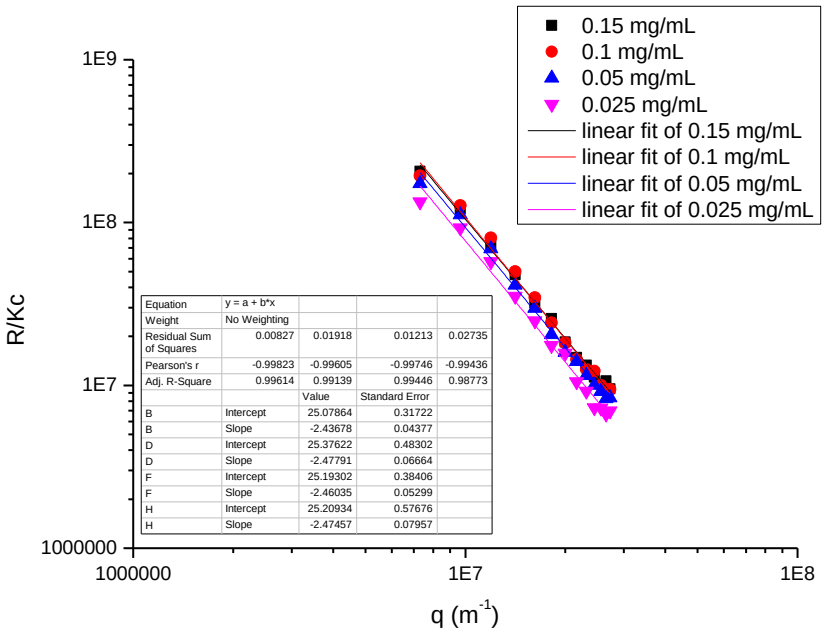

Equation	y = a + b*x			
Weight	No Weighting			
Residual Sum of Squares	0.00827	0.01918	0.01213	0.02735
Pearson's r	-0.99823	-0.99605	-0.99746	-0.99436
Adj. R-Square	0.99614	0.99139	0.99446	0.98773
		Value	Standard Error	
B	Intercept	25.07864	0.31722	
B	Slope	-2.43678	0.04377	
D	Intercept	25.37622	0.48302	
D	Slope	-2.47791	0.06664	
F	Intercept	25.19302	0.38406	
F	Slope	-2.46035	0.05299	
H	Intercept	25.20934	0.57676	
H	Slope	-2.47457	0.07957	

Figure S26. R/Kc of self-assembly of **10** in 1,4-dioxane as a function of the scattering wave vector q for different concentrations.

Section 14. AFM analysis of self-assembly afforded by **7**

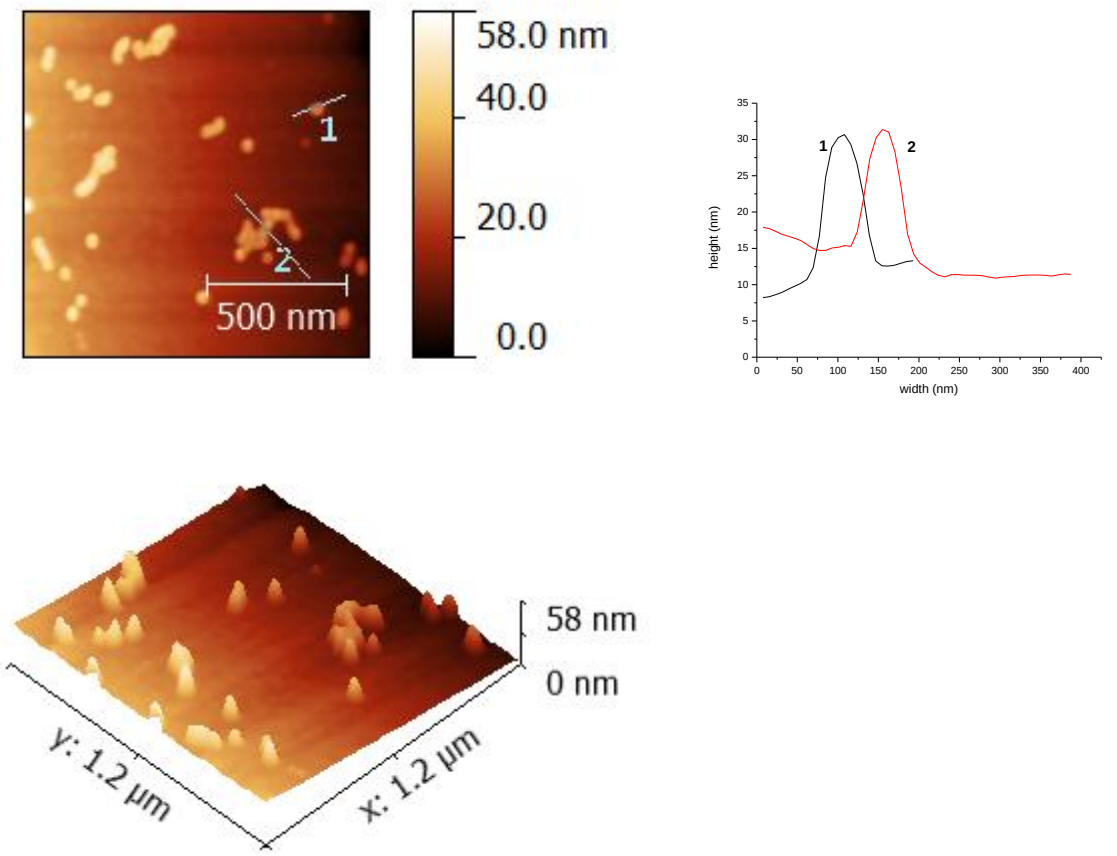

Figure S27. AFM height image (top left) and three-dimensional AFM image (bottom) of self-assembly prepared by polymerization **7** and the corresponding height profile (top right).

Section 15. AFM and SAXS analysis of self-assembly afforded by **9**

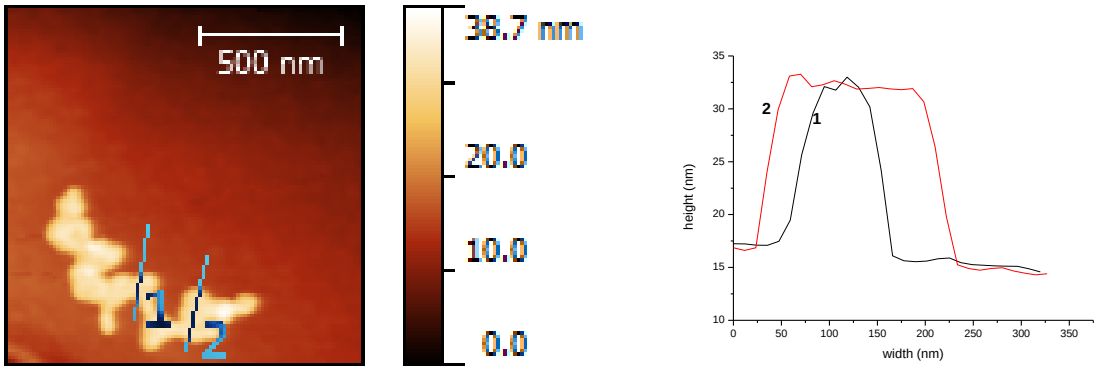

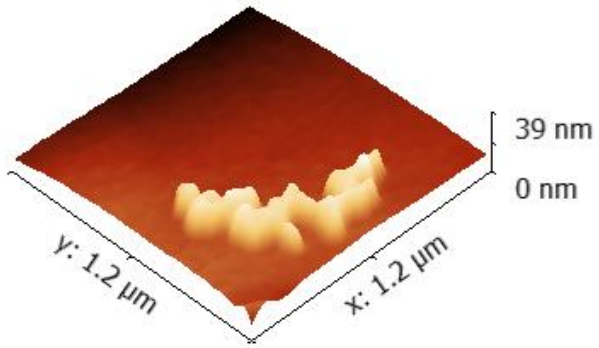

Figure S28. AFM height image (top left) and three-dimensional AFM image (bottom) of self-assembly prepared by polymerization **9** and the corresponding height profile (top right).

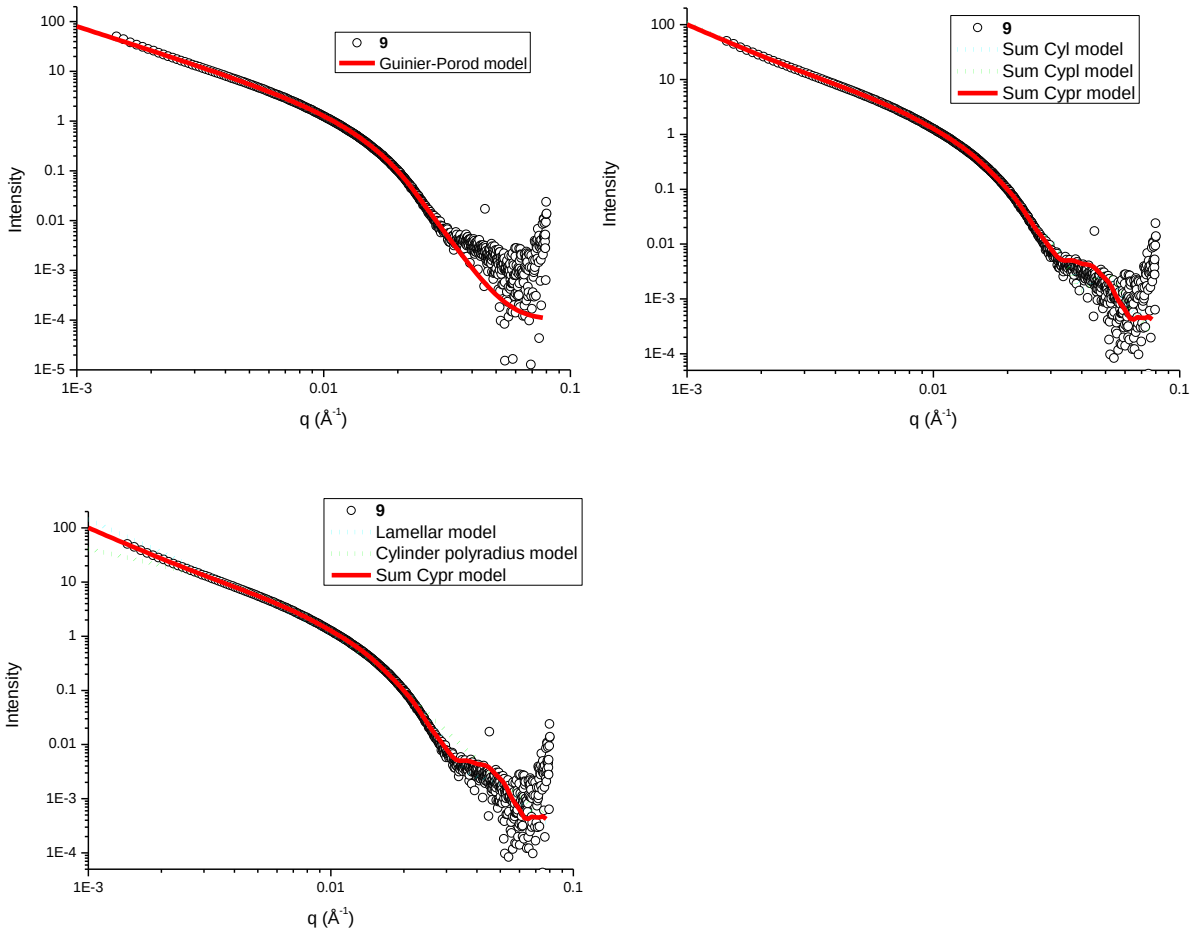

Figure S29. SAXS analysis of polymer **9**. Experimental profile and Guinier-Porod fit (top left); experimental profile and fits with different sum models: lamellar model with cylinder model (Sum Cyl model), with polylength cylinder model (Sum Cypl model), and with polyradius cylinder model (Sum Cypr model) (top right); experimental profile and fits with lamellar, cylinder polyradius and sum models (bottom).

Section 16. AFM and SAXS analysis of self-assembly afforded by **11**

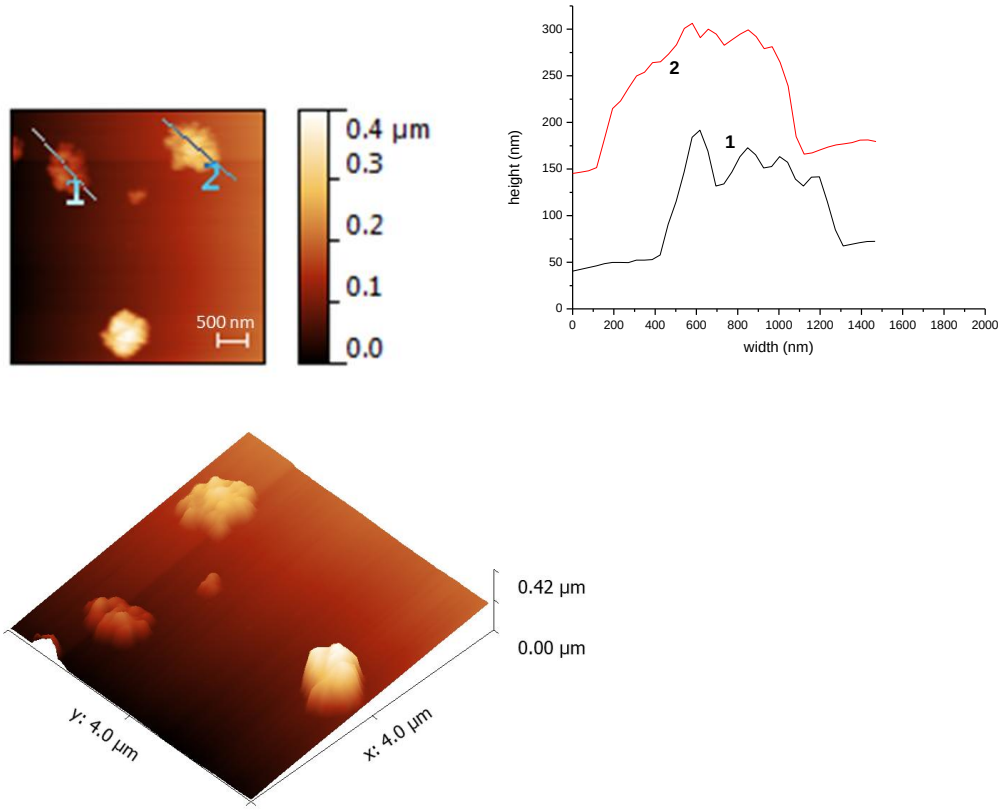

Figure S30. AFM height image (top left) and AFM phase image (bottom, scale bar 500 nm) of self-assembly prepared by polymerization **11** and the corresponding height profile (top right) performed on mica.

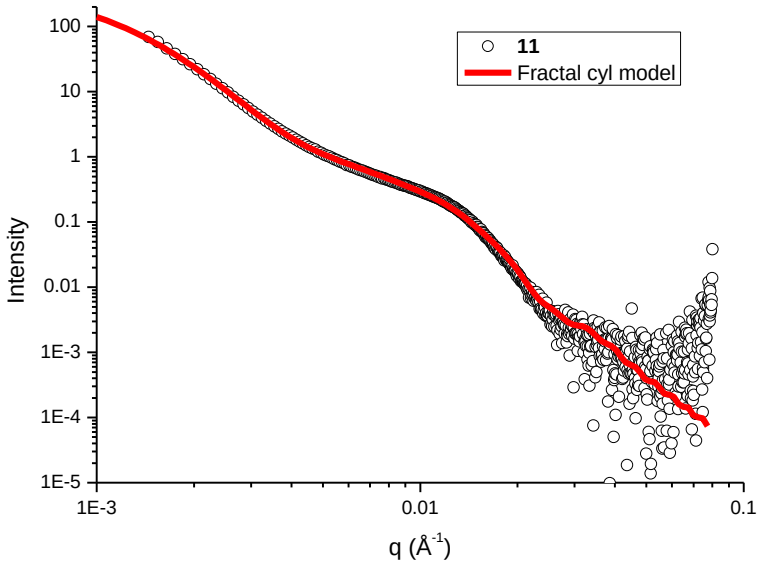

Figure S31. SAXS analysis of polymer **11**. Experimental profile and fractal fit.

Section 17. Tables of summary of results from SAXS

Table S3. Guinier-Porod model fitting data for polymers **6**, **7**, and **9** in 1,4-dioxane.

Polymer	R_g (nm)	s[a]
6	14.7 ± 0.1	0.520 ± 0.001
7	11.8 ± 0.1	0.422 ± 0.001
9	8.2 ± 0.1	1.593 ± 0.001

[a] 's' stands for dimension parameter. 0 is for sphere. 1 is for cylinder. 2 is for plate.

Table S4. Sum model fitting data for polymers **6** and **7** in 1,4-dioxane

Polymer	length of cylinder (nm)	Radius of cylinder (nm)	Radius of sphere (nm)	Volume fraction (cylinder : sphere)	Number fraction (cylinder : sphere)
6	158 ± 1	15 ± 1	18 ± 1	0.43:0.23	1:2.45
7	104 ± 1	12 ± 1	14 ± 1	0.31:0.19	1:2.51

Table S5. Size and morphology of the fitted nanostructures for **9**.[a]

model[b]	Bilayer thickness (nm)	Dispersity of thickness	Radius of cylinder (nm)	Length of cylinder (nm)	Dispersity of cylinder
cyl	17.4 ± 0.1	0.10 ± 0	16.7 ± 0.1	79.1 ± 0.3	-
cypl	17.5 ± 0.1	0.05 ± 0.02	16.8 ± 0.1	78.1 ± 0.6	0.10 ± 0.01
cypr	20.1 ± 0.2	0.05 ± 0.01	12.0 ± 0.2	80.1 ± 0.3	0.35 ± 0.01

[a]SLD solvent and morphologies were locked at 9.559 and 7.546 10^{-6} $Å^{-2}$;
[b]cyl stands for lamellar model with cylinder model; cypl stands for lamellar model with polylength cylinder model; cypr stands for lamellar model with polyradius cylinder model.